SHAFT ALIGNMENT SELF-DIAGNOSIS USING THE SMART BEARING SENSOR

(Reference NO. IJME781, DOI No. 10.5750/ijme.v163iA4.781)

C Leontopoulos, American Bureau of Shipping (ABS), **H Mouzakis**, National Technical University of Athens (NTUA), **M Petrolekas**, Metrisis Ltd

KEY DATES: Submitted: 22/10/21; Final acceptance: 11/01/22; Published 07/04/22

SUMMARY

A fully functional prototype sensor has been developed to provide new insights into vessel shaftline dynamics and which introduces real time data collection and performance evaluation. This forms part of a larger project relating to vessels' shaft alignment sensitivity under dynamic rather than static conditions, as typically required for review by the Classification Societies. The Smart Bearing Sensor was recently tested onboard a large container vessel and was shown to work with promising results. The sensor is based on strain gauge technology and has been shown to enable continuous measurement of the bearing reaction load through the strain induced onto the bearing housing by the shaft. Given the capability of continuous monitoring and recording of the bearing reaction load and shaft misalignment angle, the prototype sensor removes the need for jack-up tests for re-alignment purposes. It is envisaged that this system will allow for the earliest possible diagnosis of shaft alignment-related problems, such as bearing unloading, bearing overloading or excessive shaft-bearing misalignment. The prototype sensor could be integrated into a marine condition monitoring system that provides a more timely warning against bearing failures, particularly when compared to traditional bearing temperature sensor indications.

1. INTRODUCTION

Shaft Alignment of propulsion systems has become an increasingly important parameter in commercial vessel design during the recent years, due to an increase of shaft misalignment induced failures, causing bearing damage through wiping, vibration, and eventual vessel immobilization. This has immense consequences in the vessel's schedule, chartering and operational costs, as it requires expensive and time-consuming dry-docking operation. Most Classification Societies have been updating their Rules and Regulations, as a response measure to mitigate such risks and some of them have introduced optional Notations with optimized or so-called enhanced shaft alignment processes. The IMO's Energy Efficiency Design Index, the well-known EEDI, impacts vessel design resulting in vessels with shorter shaft lines, smaller engine rooms and more efficient propellers possessing larger diameters, slower speeds, and higher weight. Recent engine room design trends have resulted in propulsion shafting arrangements that are increasingly shaft alignment-sensitive, with lower tolerances and margins. This sensitivity heightens the risk of sterntube bearing failures. Reduced tolerance to shaft alignment sighting errors, bearing offset inaccuracies and other shaft installation errors also affect the integrity of the shafting system and can result in complete bearing wiping resulting in vessel propulsion immobilization. Such incidents have greatly increased, particularly in the period of 2013-2017 (Leontopoulos *et al.*, 2020).

Figure 1. Engine room shaftline arrangement for a Container vessel

The need to address shaft alignment under running or dynamic operational conditions, as opposed to traditional static conditions, has become more apparent, as the vessel's wake field, interacting with the propeller or even with Energy Saving Devices (ESD), greatly influences the bearing loads, the shaft-bearing misalignment angles, and the shafting system in general. This demand has led to the development of the vessel's shaftline and powertrain condition monitoring systems, which can diagnose faults including vibration and shaft alignment-related problems. There exist a few commercial condition-monitoring systems, which would include a combination of installation of displacement sensors, temperature sensors or strain gauges fitted on the shaftline, providing some visibility onto its behaviour

under actual vessel operational loading conditions; however, these can be expensive and require specialized personnel to interpret the output data. Such condition monitoring systems would involve powerful data acquisition systems combined with intelligent statistical data and post-processing modelling.

In 2017, ABS began efforts to research the practical application of a sensor, called the "Smart Bearing Sensor", in collaboration with the Laboratory of Earthquake Engineering of the National Technical University of Athens (NTUA) and Metrisis Ltd, leading to the development of a simple prototype sensor able to measure and monitor the bearing load and the shaft-bearing misalignment angle through the bearing housing strain induced by the shaft. The purpose of this project was to devise a measurement protocol with strain gauges on a marine intermediate shaft bearing housing to measure the bearing reaction load. Effectively, this would convert a bearing housing into a weighing machine, possibly dispensing with the need of shaft re-alignment inspections, as required by the Classification Rules and Regulations. In this way, the bearing reaction load can be measured continuously in both static and, most importantly, dynamic operational conditions, while the vessel operator will be able to assess if an intermediate bearing is overloaded or unloaded at any time. A strain gauge circuits configuration is used for the recording of the strain, which is then mapped onto actual bearing load and shaft misalignment angle through a set of predefined equations (Leontopoulos *et al*., 2020). Following its development, the prototype sensor has been successfully tested to-date in three vessels during sea trials (Figure 1 and Figure 2).

Figure 2. Engine room shafting arrangement showing the aft of the two intermediate bearings, where the Smart Bearing Sensor was installed, calibrated, and tested.

2. INITIAL EXPERIMENTAL AND NUMERICAL INVESTIGATION

To determine whether the strain induced on an intermediate bearing housing can be measured and mapped onto bearing load, an experimental investigation accompanied by Finite Element Modelling (FEM) was undertaken. This entailed understanding the actual possible strain magnitudes to be practically detected and measured on a bearing housing, as well as the steel frame locations of the strain gauges. A Wartsila intermediate bearing housing was used for experimental purposes. A replica of an intermediate shaft was installed inside the bearing housing. The shaft was trimmed at the top so that load from a hydraulic actuator could be exerted onto the shaft in a steady manner without risking rotation and slip.

A stiff external steel "Pi"-shaped loading frame was used upon which a hydraulic actuator was affixed, as shown in Figure 3. A downward force was applied along the main vertical axis of the specimen. Eccentric loads were applied to simulate shaft eccentricities by moving the axis of the actuator relative to the main axis of the specimen in increments of +50mm to +200mm and -50mm to -200mm. The applied force was ramped from zero to a maximum value of 80kN at a rate of 10kN/min. The loading rate for the specific bearing size and type used in the laboratory experiment was such, so that to simulate typical loading rates experienced in reality. No particular sensitivities are expected to be induced by the loading rate. The resistance of the strain gauges was 120.4Ω and the gauge factor k= 2.11. Three lead wire connections were applied, and a quarter Wheatstone bridge configuration was adopted. The strain gauges used were suitable for steel and for temperature compensation. Ten (10) different locations were selected to measure the strain, including the bottom plate of the intermediate bearing housing, see Figure 4. All strain gauges installed recorded clear signals and were used in the experimental investigation (Mouzakis, H, 2016). The influences of cross-sensitivity to transverse or horizontal directions were also considered and studied, although their influence was regarded as practically insignificant for the typical loading profile of the bearing. Typical horizontal loading values produced insignificant strain onto the bearing housing or onto the housing bottom plate, that could be amplified to map onto bearing load.

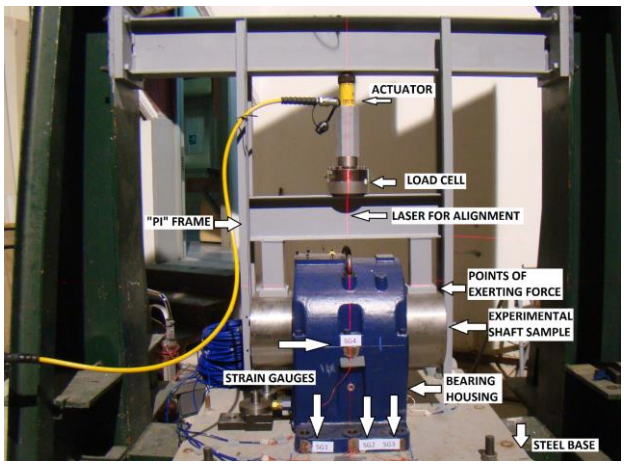

Figure 3. Experimental Arrangement with Intermediate Bearing Housing Strain Gauges, Simulating Intermediate

Bearing Load in Laboratory Conditions, (Leontopoulos *et al.*, 2020)

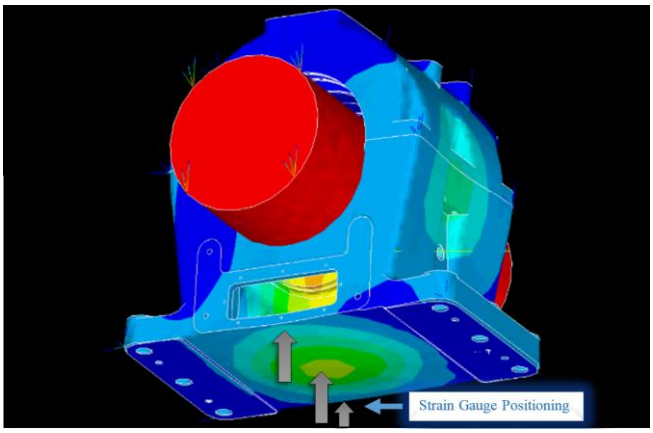

Figure 4. Strain Gauges installed at the centre of the bottom plate of the bearing housing being the most strain sensitive location to shaft loading, as per laboratory measurements and FE bearing housing analysis (Leontopoulos *et al.*, 2020).

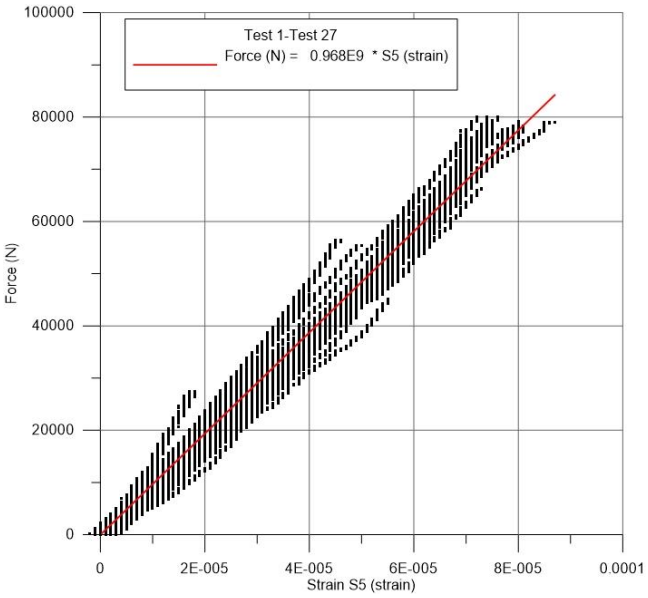

Figure 5. Bearing Load (Force) versus Strain at the Centre of the Bottom Plate of the Bearing Housing Collected for All Tests, (Leontopoulos *et al.*, 2020)

Two displacement transducers were used adjacent to the bearing positions to record the rotational angle of the shaft at the ends of the bearing. The shaft centre-line inclination was calculated from the difference of the displacements measured by these two sensors. Several tests were carried out simulating a load exerted by the shaft onto the bearing housing and recording the strain at a number of selected locations. The shaft misalignment angle and strain distribution changes were also recorded. Using a sophisticated data acquisition system, data was acquired at a rate of 50 Hz. A low-pass filter with a 1 Hz cut-off frequency was also used. The experiments and the Finite Element Model revealed that the most sensitive locations were primarily at the bottom plate of the bearing housing. The objective of these experiments was then to correlate the applied load with the measured strain, as well as the applied loads at various eccentricities versus the shaft misalignment angle and the distributed strain. Curve-fitting techniques were employed to provide the appropriate equations for the mapping of strain versus bearing load, see Figure 2.3. The red line shown in figure 5 is not an “average line” of the tests but the result from one single test, where the shaft loading is fully symmetric. For that test the variance in linearity was insignificant. While the lab testing reported a sensitivity of 0.968 kN:microstrain, the sensitivity for the installed ship trial system was reported at 0.103 kN:microstrain. Such factors are specific to the structure and size of the bearing housing. It was equally confirmed through the calibration process using jack-up tests, that a linear response of system output to bearing load remained.

The correlation between the numerical and experimental results was satisfactory, albeit a degree of uncertainty existed due to non-linearities that were potentially unaccounted for. Potential sources of non-linearities included friction between various surfaces and edges within the bearing housing structure. The FEA model contained contact elements on all mating surfaces (e.g. upper and lower shell, internal plates, etc.), making the model as realistic as possible. FEA models were subsequently developed for similar intermediate bearing arrangements and showed that the curve-fitting equations, mapping the strain onto load showed all consistent trends. Three different intermediate bearing cases, both from Wartsila and Kemel were experimentally investigated through FEA modelling, correlated with measurement tests, both in the laboratory and onboard vessels and albeit non-identical bearing housing designs, they demonstrated the same linear strain-gauge behaviour while, any deviation from linearity was considered insignificant amongst the three different cases.

It must be noted that the prototype sensor arrangement has not been tested onto intermediate bearing pedestals with top plates, as it would not be possible to fit and install the sensor due to lack of suitable space. The possibility to remove/withdraw the intermediate shaft and lift the bearing housing, in order to access its bottom plate, would have been impractical for a sailing vessel and could only take place at suitable dry-docking. The initial calibration process through the jack-up test includes effects from the ship foundation in the process of mapping the strain onto the bearing reaction load through the equation coefficients.

3. APPLICATION ONBOARD VESSEL

Once the concept was proven in the laboratory, the prototype sensor was developed and installed on board three vessels. In this case, we examine the Smart Bearing

Sensor fitted onto a 9,100 TEU container vessel, as part of its testing under real-life conditions. The strain gauges were installed at the bottom of the bearing housing plate in two half-bridge circuits and were connected to the Smart Bearing Sensor box installed at the bottom side of the bearing housing. The strain gauge positioning is dictated by the experimental and FEA data obtained from several bearing housing cases and through work performed in the University laboratory. The Smart Bearing Sensor box is then connected to a Display Unit (DU) or a laptop.

Alternative to a Display Unit, the measured values could be transmitted to the engine control room through ethernet or wirelessly and be integrated into the vessel's monitoring system. The Smart Bearing Sensor box consists of a National Instruments NI 9219 Universal Input Module, capable of providing excitation and of measuring full and half strain Wheatstone bridge resistances of either 120 or 350 Ohms, through a multi-channel data acquisition system, see Figure 6. For the current prototype sensor, the increase signal to noise ratio for the installed bridges was achieved by installing half bridges of 350 Ohms each.

Figure 6. NI-9219 Module (Copyright National Instruments) on the left, Laptop Display in the middle, Prototype Independent Display Unit (DU) on the right

The sensor data acquisition software provides three output values every two seconds: the bearing load in tons, the shaft misalignment angle in mrad, and a bearing status indication.. A pilot Bluetooth receiver-transmitter protocol was used to display the values both on a prototype display and also on a prototype beta-tested application on an Android mobile phone. The Display Unit (DU) shows, in addition to the two values of bearing load and shaft misalignment angle, a "bearing status" indication as "OK" or as "NOT OK" (Alarm). The Alarm options infer to "overload", "unload" and "excessive misalignment angle" for misalignment values exceeding 0.3 mrad. All measured values are recorded into the sensor internal memory card and can be retrieved for further processing, e.g., for a reverse shaft alignment calculation and subsequent diagnosis.

Although the Smart Bearing Sensor is meant to eliminate the need for shaft alignment jack-up tests, an initial calibration is required to determine the coefficients of the equations for the conversion of the bearing housing strain to bearing load in tons and the misalignment angle in mrad. This is achieved by performing jack-up tests lifting the shaft inside the bearing gap and recording the bearing housing strain distribution when the shaft is resting on the bearing housing and until the bearing housing becomes unloaded. The values of strain and jack load are recorded in order to determine the equation coefficients relating the bearing load and the strain at the location of the bearing housing. Jack-up tests are also performed to calibrate the misalignment angle by moving the jack position at a specified distance further away from the bearing centre and initiating a shaft misalignment angle. The bearing housing deformation is then captured by the strain distribution, as measured by the strain gauges array installed at the bottom of the housing. The strain values are then mapped onto misalignment angle values in mrad for the determination of the equation coefficients. During the calibration process, the bearing load curve data is acquired via the available channels, that is, data coming from a load cell, two displacement sensors adjacent to the bearing housing and strain gauge circuits, associated with two channels.

After calibration, the sensor remains fully operational. Correlation amongst the calculated values from the original Class-approved shaft alignment calculation report, as well as with respect to the original jack-up test values during the original vessel's sea trials, is found satisfactory for the loading condition measured during the calibration. This means that the bearing load is in accordance with the design values presented in the original shaft alignment calculation report, and accordingly to bearing load measurements during the vessel's sea trials. The jack correction factor is taken into account in the measurement of the bearing load, as per the shaft alignment calculation for the specific arrangement. The sensitivity factors of the reported sea trial system were internally calculated by the bearing sensor software during the calibration process at 0.103. Such factors are specific to the structure of the bearing housing. It was confirmed through the calibration process using jack-up tests, that a linear response of system output to bearing load existed.

4. SMART BEARING SENSOR SEA TRIAL ONBOARD CONTAINER VESSEL

Upon completion of set-up and calibration, the container vessel commenced sea trial movements, starting with manoeuvres inside the anchorage area to reaching cruising speed and performing turns in the open waters on its way to the destination port. Such manoeuvres demonstrate the fluid structure interaction amongst the propeller, rudder and induced wake field, stimulating a movement of the shaftline and thus, exhibiting a recordable change in bearing loads during operation. It is well known that significant vertical and transverse propeller forces and moments can be exerted from the propeller onto the shaftline during vessel turning (Vartdal, BJ, Gjestland, *et al.*, 2009), (Broglia, R, Dubbioso, G *et al.*, 2012), thereby, affecting the bearing loads, mainly in the vertical direction. During this time, the sensor was set to continuously record the

intermediate bearing load and the misalignment angle. The values for shaftline RPM and rudder angle were also obtained from the vessel's engine control room data acquisition system. Time stamping was synchronized between the prototype sensor's data acquisition unit and that of the vessel, to overlay quantities for improved understanding. The shaftline arrangement of the commercial 9,100 TEU container vessel consisted of a slow-speed, 9-cylinder engine at 80 rpm MCR, two intermediate shafts and one tailshaft with a 6-bladed fixed pitch propeller. At the time of the testing of the sensor onboard the vessel, there was only one available prototype sensor, and this was installed onto the aftmost intermediate bearing, the one closer to the propeller.

Figures 7 and Figure 8 show graphs of the intermediate bearing load variation, overlaid with the rudder angle variation and shaftline RPM against time, during the sea trial manoeuvres. It is noted that at time 12:14, the vessel performs a manoeuvre with a 35-degree port turn together with an RPM increase from zero to 24. The decrease in intermediate bearing load is likely to be due to a combination propeller eccentric thrust and simultaneous large rudder turning, both influencing the sudden forces onto shaftline, in conjunction with a sensitivity to rotational friction of the shaft in the bearing. This phenomenon has been observes on all vessels tested with the experimental sensor installed at their intermediate bearings. At 12:32 the rudder angle changes from port 35 to starboard 35 and together with an increase in RPM to 40 RPM. An intermediate load variation can be observed between 12:33 and 12:39 and onwards as a result of the propeller and rudder interaction with water, causing lateral forces onto the shaftline. It is also noted that the bearing load variations between time stamp 12:46 and 13:12 lie between 19 to 21 tons and these are mainly caused by the rudder movement during this period of time, varying from 0 degrees to port 10 degrees, to port 35 degrees and back to zero. Such maneuvers demonstrate the fluid-structure interaction amongst the propeller, rudder and induced wake field and the influence on the shaftline dynamics.

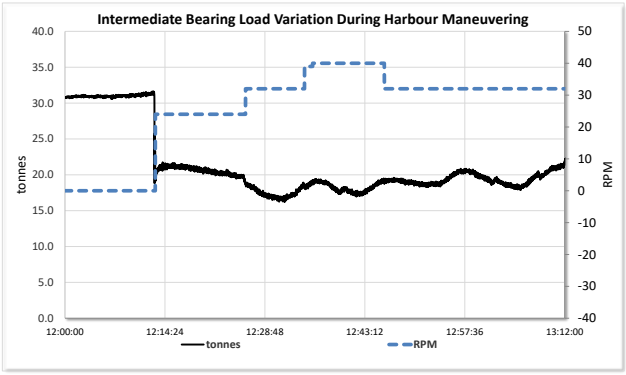

Figure 7. Intermediate Bearing load variation against shaftline RPM

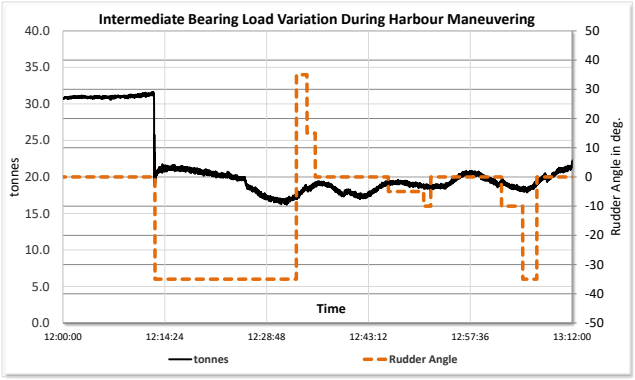

Figure 8. Intermediate Bearing load variation against rudder angle

Similarly, Figures 9 and 10 show bearing load variations between time stamp 13:12 and 13:40. During this period, there are astern vessel movements, which at 13:15 appear to cause temporary bearing load increase and were combined with onwards port and starboard 35-degree turns.

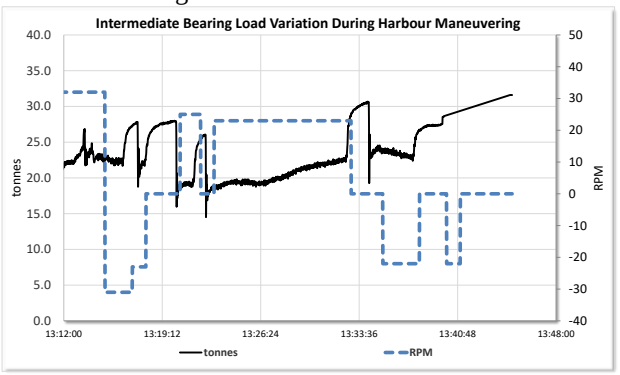

Figure 9. Intermediate Bearing load variation against shaftline RPM

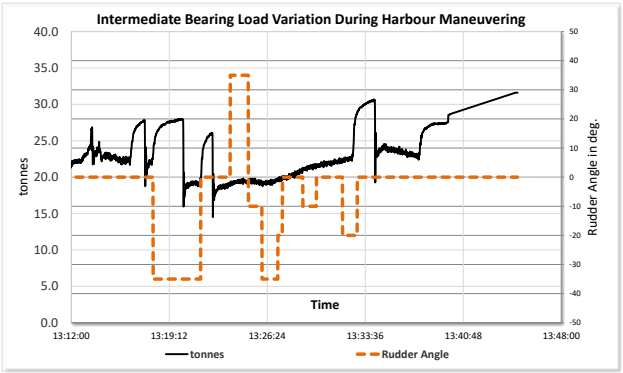

Figure 10. Intermediate Bearing load variation against rudder angle

These resulting propeller loads (forces and moments) involve transitory phases during vessel turning, where such transient loads are quite difficult to predict with satisfactory accuracy even by the most advanced CFD

calculations. Subsequent rudder angle changes combined with changing RPM, including ahead and astern settings, appear to cause measurable load fluctuations onto the intermediate bearing in this shaftline. Large vessels turns at high speed (MCR), such as that of the subject 9,100 TEU container vessel are expected to cause substantial shaftline forces, thus causing significant bearing load changes. However, operational practices allow port/starboard angle variations no greater than 10-degrees. At the request for a high-speed turn to provoke a shaftline disturbance, hence causing measurable bearing load variations by the prototype sensor, it was noticed that a delay/lag is demonstrated in the bearing load variations quite some time after the original "disturbance", unlike in the case of slower speed manoeuvring, see Figure 11. This is likely to relate to the fluid-structure interaction and the associated caused lag observed in the heading changes of the vessel due to its size and inertia. Similarly, the misalignment angle variation follows the bearing load changes, albeit at insignificant values for the bearing contact, as shown in Figure 12.

Due to simultaneous combinations of rudder and shaft speed, as were dictated by the vessel heading changes and considering the vessel type and size, it is not possible to isolate and quantify the influence of the above dynamic effects on the shaftline, due to time and vessel trade constraints, nor it is the purpose of this study, which is rather to highlight the R&D concept of the prototype sensor technology and its performance. The results in figure 12 may likely be influenced by vessel previous -to the presented times- movements of zigzag turns, as dictated by the then local traffic also influenced by weather and sea currents. Given the type and the size of the vessel, the lag between a rudder turn and the final vessel heading as a result of this turn, even at high RPM, it is possible that such "delayed" shaftline forces can influence the intermediate bearing accordingly. This apparent "lag" phenomenon between a turn and the final intermediate bearing reaction has not been observed in smaller sized vessels and can be a subject of further research.

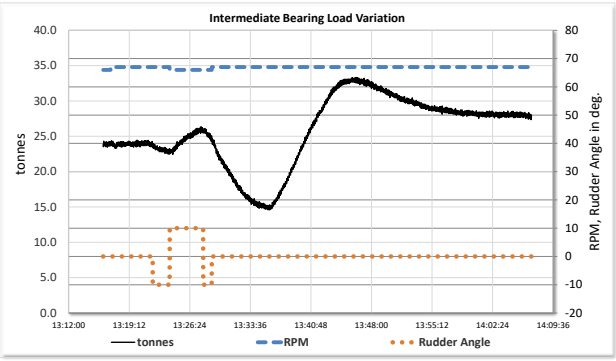

Figure 11: Bearing Load variation/disturbance versus shaftline RPM and rudder angle

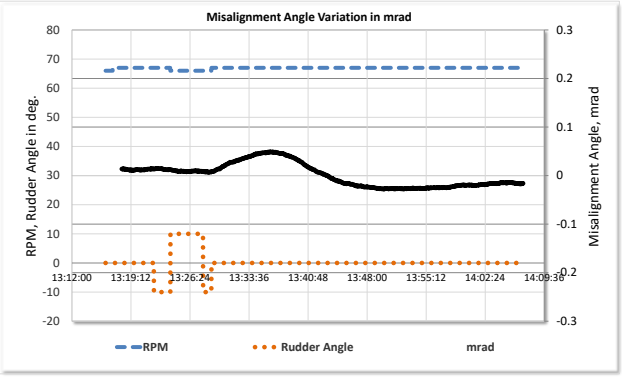

Figure 12. Misalignment Angle variation in mrad versus shaftline RPM and rudder angle in degrees. Acceptable limits are +/- 0.3 mrad

The majority of vessel operations involves cruising in a straight-ahead course at design speed while in open waters. In these conditions, the shaftline stabilizes without being influenced by changes in fluid-structure interaction. To this end, bearing load fluctuations are not expected and therefore the bearing load value is to remain constant, as was measured by the prototype sensor, see Figure 13. These constant bearing values are expected to change only between ballast and laden conditions, where hull deflections would alter the bearing offsets, or in the case of bad weather conditions, where propeller forces, combined with vessel movements, such as rolling and pitching could influence the shaftline bearing reactions.

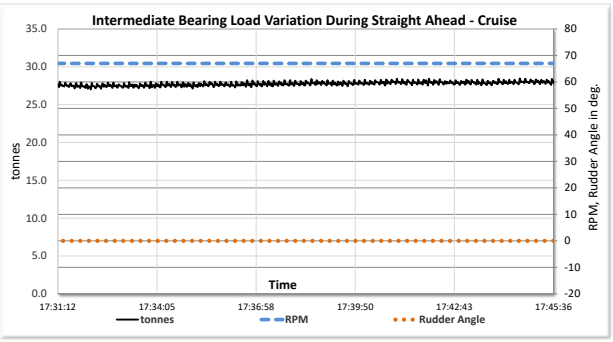

Figure 13. Intermediate Bearing load variation against rudder angle and shaftline RPM during open waters cruise

5. REVERSE ANALYSIS AND DIAGNOSES

A beam-based Finite Element computer model is typically used for the assessment of the shaft alignment calculation. The bearings are modelled as single points of support and the bearing reactions are determined. The bearing reaction values are verified to be within the bearing manufacturers' limits; see Figure 14. The subject shaft alignment computer model, used originally for the vessel's shaft alignment Class approval, can also be used for reverse calculation purposes. The bearing load measured values can be fed back into the computer

model and through a reverse model iterative calculation, the actual shaft deflection slope throughout the shaftline arrangement can be determined, under certain assumptions: These assumptions would include jack-up tests with satisfactory correlation against calculations for prescribed static conditions for all measurable bearings to ensure a linear model validation and known propeller forces through CFD analyses for a previously validated and calculated hull deflection vessel loading condition (ballast, laden, etc.) at steady state. That is, similar to the same concept as the shaft strain gauge reverse engineering analysis. Thus, the bearing loads of the adjacent bearings can be determined even if not measured by the Smart Bearing Sensor or otherwise, when assuming that any change occurs only due to the variation of propeller loads.

In this case, the information fed into the computer model comes from the Smart Bearing Sensor. This includes bearing load and misalignment angle at specific time steps during the vessel's operation and from a specific bearing. Assuming the same vessel loading condition between the model and the actual sea trial (e.g. fully laden condition), the effect of the propeller loads onto the shaftline bearings and onto the intermediate bearings can be investigated. Figure 14 shows a typical shaftline FE model used for plan approval purposes.

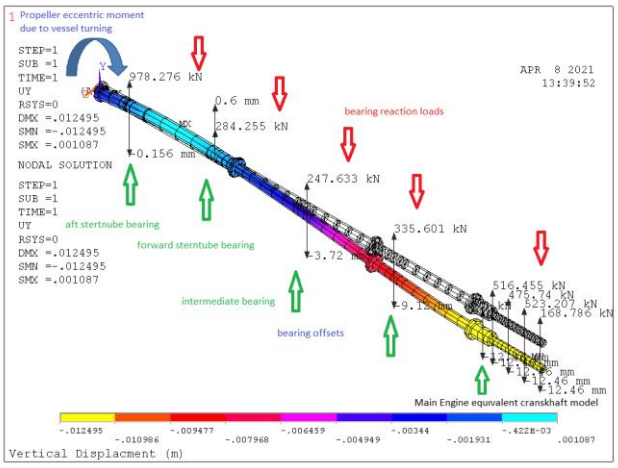

Figure 14. Shaftline Finite Element Model for shaft alignment showing calculated bearing reactions and corresponding bearing offsets

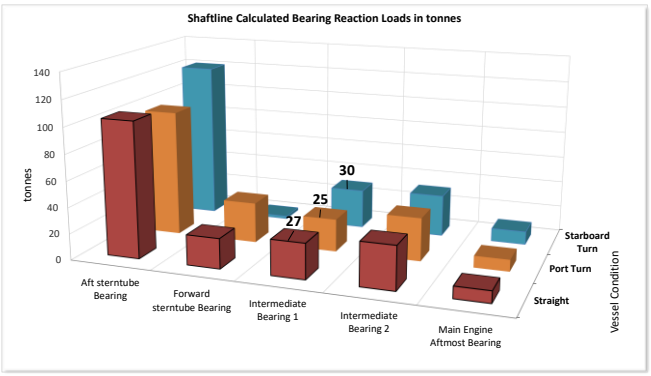

Figure 15. Shaftline calculated bearing reaction loads for straight ahead, starboard turn and port turn at vessel MCR (quasi-static/steady-state condition through reverse engineering). Prototype sensor installed at Intermediate Bearing 1

Table 1. Calculated/Predicted versus Measured intermediate bearing reaction load during sea trials (quasi-static/steady-state condition through reverse engineering)

Intermediate Bearing Reaction Load, tons	Straight	Starboard Turn	Port Turn	Allowable Limits
Measured by the Smart Bearing Sensor	27	32	15	0 - 57.5
Calculated considering propeller eccentric moments	27	30	25	

Figure 15 shows the calculated shaftline bearing reaction loads for three vessel conditions, namely, "laden – straight", "laden – port turn" and "laden – starboard turn" with emphasis on the aft intermediate bearing, where the Smart Bearing Sensor had been installed. The three conditions consider the hull deflections under the "laden" condition, as well as the steady-state propeller eccentric moments transmitted onto the shaftline during vessel turning, in accordance with the ABS ESA Guide (Enhanced Shaft Alignment, ABS Guide, 2018). According to this Guide, it is statistically observed that for single-screw vessels performing a starboard high-speed turn, the propeller wake interaction causes a downward bending moment, causing the shaft to pressurize the aftmost edge of the bearing and unload the forward sterntube bearing. Similarly, for a port turn, an upward bending moment would relieve large vertical pressures from the aftmost sterntube bearing and re-distribute loads by transferring lesser loads to the forward sterntube bearing and intermediate sterntube bearings. These bearing load redistributions can be simulated in the FE computer model and correlation can be shown with the bearing reaction loads, see Table 1.

6. CONCLUSIONS

Testing the Smart Bearing Sensor on the intermediate bearing of a 9,100 TEU Container's 35m-long shaftline

allowed for the continuous measurement of the bearing load and misalignment angle under all shaftline operational conditions. Even though the intermediate bearing is further away from the propeller with a forward and an aft sterntube bearing in between, one can infer, through reverse calculations, the bearing load re-distribution caused by the propeller loads, due to the demonstrated intermediate bearing load and misalignment angle variations. Due to time and vessel trade constraints, the sea trial measurements of the intermediate bearing dynamic load have not been verified by separate measurement, such as shaftline strain gauging, however, similar verifications have been satisfactorily achieved in previous test cases (Leontopoulos *et al.*, 2020).

Both unloading and overloading of a bearing are undesirable conditions and can cause either shaft whirling for the unload case or overheating and bearing damage for the overload case. With the current system, the vessel operator can not only observe the bearing loads at all times but can also "undo" a vessel movement that is suspected to have caused an unload or overload or in general an undesirable shaftline disturbance, by performing a corrective action. This can also be reflected to the various vessel loading conditions, varying from light ballast to full scantling draft, where the hull deflections affect the bearing offsets and the overall shaft alignment.

Therefore, a system of Smart Bearing Sensors can enable the operator to take appropriate measures to avoid unacceptable bearing temperature rises or shaftline vibration or whirling, by performing corrective movements, ensuring a healthy envelope of operation. The measured values from the sensor can be used to reverse engineer a validated shaft alignment model to estimate the bearing load re-distribution; and, for increased accuracy, more sensors can be installed to reduce the number of theoretical solutions found through reverse engineering. Furthermore, such sensors can be used in conjunction with validated models in machine learning technologies, as well as to establish an envelope protection against damage, failure, or even premature bearing wear. Application of this technology to the sterntube bearings will make for an integrated system that will provide enhanced vessel protection through an efficient, practical and meaningful shaftline condition monitoring system.

The installation of the smart bearing sensor on the intermediate bearings is the first step of a potentially promising innovative technology concept for onward application onto the sterntube bearings. The present project is to be expanded onto the installation of pertinent strain gauge arrangements embedded into sterntube bearing bushes through OEM, making the bushes themselves "Smart Bearings". Any results/experiences drawn from the current applications, such as Bluetooth technology, data acquisition protocols, strain amplification factors and electronic noise interference, are likely to assist in these future efforts for a continuous integrated monitoring of the vessel's shaftline.

The accumulation and understanding of this newly found knowledge and accumulating experience will further lead to updated Rules and safety factors assessing the shaft alignment dynamic/running conditions, which are the conditions under which actual bearing failures take place. Shaft Alignment-sensitive shaftlines, such as those with single sterntube bearing or shaftlines with water lubricated bearings, or long and slender shaftlines with heavy propellers may benefit most from such innovative monitoring systems, minimizing the risk of bearing failure and the subsequent consequences of vessel immobilisation.

7. ACKNOWLEDGEMENTS

The authors would like to thank the management and personnel of Messrs Capital-Executive Ship Management Corporation for their contribution in the research and for their kind offer to allow R&D staff from ABS and NTUA to install and test the prototype sensor installation on board the Container vessel M/V "CMA-CGM URUGUAY", IMO 9706310. In addition, the authors would like to thank Mr Simos Asimakopoulos, Senior Research Engineer at the Laboratory for Earthquake Engineering of NTUA for his participation in the development and application of the system.

8. REFERENCES

1. LEONTOPOULOS, C, MOUZAKIS, C, PETROLEKAS, M, *Smart Bearing Sensor*, SNAME, Journal of Ship Production and Design, 2020, Vol.36, No1
2. LEONTOPOULOS, C, 2016, *Propulsion Perspective, Shaftline Optimization, Aligning Goals*, The Marine Professional, IMarEST, London, UK
3. American Bureau of Shipping, *Shaft Alignment Guidance Notes*, 2018, ABS, Spring, Texas, USA
4. American Bureau of Shipping, *Enhanced Shaft Alignment Guide*, 2018, ABS, Spring, Texas, USA
5. MOUZAKIS, H, 2016, *Investigation of the Behavior of a Bearing Housing - Pedestal Under Static Conditions,* National Technical University of Athens, 2016, ABS Internal Report, Athens, Greece
6. LEONTOPOULOS, C, 2016, *Smart Bearing Pedestal*, ABS Report TR-2016-3442265, ABS, Houston, USA

7. PETROLEKAS, M, 2016, *Strain Gauge Sensor Unit For Bearing Housing Strain Monitoring Theory and Praxis*, Internal Report, Metrisis Ltd, ABS Internal Report, Athens, Greece
8. VARTDAL, BJ, GJESTLAND, et al, DnV-GL, 2009, *Lateral Propeller Forces and their Effects on Shaft Bearings*, First International Symposium on Marine Propulsors, Trondheim, Norway
9. BROGLIA, R, DUBBIOSO, G, et al, 2013, *Simulation of Turning Circle by CFD: Analysis of different propeller models and their effect on maneuvering prediction*, Appl. Ocean Res. 2013, 39,1-10
10. ANSYS Inc, 2019, *Mechanical APDL, Mechanical User's Guide*, ANSYS v.19.1, Canonsburg, Pennsylvania, USA
11. ABS Shaft Alignment software v3.1, ABS Spring, Texas, USA
12. LEES AW, MOTTERSHEAD K, FRISWELL MI, 2004, *Nonlinear Dynamics of Production Systems*, Wiley-VCH, Weinheim, Germany

